Geothermics 79 (2019) 1–13

Contents lists available at ScienceDirect

Geothermics

journal homepage: www.elsevier.com/locate/geothermics

Use of 3D electrical resistivity tomography to improve the design of low enthalpy geothermal systems

Ignacio Martín Nieto*, Arturo Farfán Martín, Cristina Sáez Blázquez, Diego González Aguilera, Pedro Carrasco García, Emilio Farfán Vasco, Javier Carrasco García

Department of Cartographic and Land Engineering, University of Salamanca, Higher Polytechnic School of Avila, Hornos Caleros 50, 05003, Avila, Spain

ARTICLE INFO

Keywords:
Electrical resistivity
Thermal conductivity
Granite type rocks (adamellites)
Design of the well field

ABSTRACT

In designing low enthalpy geothermal systems, the ideal location and length of the boreholes in the well-field is the key to improve the performance and reduce the costs of the installation. The correct assessment of the heat conductivity of the ground (λ) plays also a very important role in estimating the amount of energy that we are going to be able to obtain from the subsoil and the ideal pace of the process. In low enthalpy geothermal installations based on granite type environments is especially important to improve the information we have from the subsoil at a small scale. This is due to the great horizontal variation we can find on this kind of terrain.

Electrical conductivity ($C = 1/\rho$, ρ = resistivity in ohm meters) can be related to thermal conductivity (λ) of many rock types (Directive (EU), 2019) (see Robertson, 1988). We show that a 3D electrical resistivity survey can be used as a proxy for λ in terrain with weathered and solid granitic rock. Knowledge of λ is essential for the design of efficient ground source heat pump systems that use vertical wells for closed-loop systems. Shorter well lengths are accomplished if wells are in solid granite with high λ. Furthermore the electrical resistivity survey identifies low density, clayey subsurface materials that may require specialized drilling methods. Project cost savings can result from shorter borehole lengths, number of holes, and correct drilling methods.

1. Introduction

In the current context of greenhouse gas emissions reductions policies carried out by the European Union (Directive (EU), 2019), and many other countries, the use of electricity for heating purposes is taking more and more prominence. Low enthalpy geothermal systems can play a relevant role given its advantageous features:

- Great efficiency. These systems do their work with coefficients of performance (*COP, performance of heat pumps is usually expressed as the ratio of heating output or heat removal to electricity input*) starting in 4 and up in the majority of cases.
- Possibility of implementing low enthalpy geothermal systems in large geographical areas with decent technical and economic performance (Blázquez et al., 2017a).
- Continuous improvements in both, the design and the price of these systems, which is making them increasingly competitive.

The initial investment for low enthalpy geothermal installations is still quite high compared with other heating systems based on natural gas or diesel oil to name a few (Blázquez et al., 2018a), this is the main reason inhibiting widespread use of geothermal heat pump systems compared to conventional heating methods. Improvements on the design of the well field area can be very significant in the attempt to reduce the initial cost of the project.

One of the main parameters to design a low enthalpy geothermal system in a precise way is the thermal conductivity (λ) of the ground where the installation will take place. Meanwhile the whole majority of the other parameters can be calculated or esteemed more or less in a direct way (energy needs, heat pump nominal power, etc.), usually the λ is not easy to assess precisely enough. This obliges the designer to oversize the well field of the system, increasing the initial investment, due to the fear of being short in the estimation of the necessary length of the geothermal circuit. Good conductivity is necessary for utilizing ground as a heat source or sink. To be able to estimate, as accurately as possible, the thermal conductivity of the ground (λ) is also key in the design of other underground structures such as: nuclear waste underground repositories (which must diffuse heat generated by the radioactive waste), etc (Sundberg et al., 2009).

This paper is an example of the use of geophysical properties of

* Corresponding author.
E-mail address: nachomartin@usal.es (I.M. Nieto).

https://doi.org/10.1016/j.geothermics.2019.01.007
Received 12 September 2018; Received in revised form 12 December 2018; Accepted 9 January 2019
Available online 12 January 2019

granite type rocks (adamellites in this case) in order to improve the design of the well-field from a low enthalpy geothermal system. We will estimate the thermal conductivity of the ground as well as finding the best places to locate the wells needed. All this will be decided using data from the 3D Electrical resistivity tomography (*ERT*), supported by some lab determinations of thermal conductivity (λ) and electrical resistivity (ρ) of samples from the project´s area.

Nowadays, the most respected essay, in order to obtain an accurate value of the average bulk conductivity (λ), is the Thermal Response Test (*TRT*) (Sanner et al., 2003). However, it is much more expensive than our proposed method, and it is much more local by nature. Indeed, when you obtain λ from this test, you only know this value for the terrain surrounding the borehole tested (Signorelli et al., 2007; Sanner et al., 2005).

Many devices are capable of measuring the thermal conductivity of a certain material from samples in the laboratory (Blázquez et al., 2017b), these devices do not consider the whole rock formation conditions in the thermal conductivity results (Liou and Tien, 2016), so they do not represent the thermal conditions we can find in the ground (Kukkonen and Lindberg, 1995).

We will proceed using the electrical resistivity data of the adamellites, collected from the tomography, to estimate the thermal conductivity and the compactness distribution of the rock mass in the location area (Popov et al., 2003).

Estimation of rock density from Electrical Resistivity (ρ) has an additional benefit of locating areas of altered rock that could present drilling problems. Drilling difficulties may be mitigated by choosing an appropriate boring method for the predicted rock material (i.e. mud rotary, percussion, coring, etc.) (Fig. 1).

In the process of alteration of the granite type rocks, and the adamellites in particular, a relation between electrical resistivity on one hand and thermal conductivity and alteration grade on the other hand can be established. This means that by using the data from the electrical tomography we can assess those parameters in order to improve the design of the geothermal system.

With the data collected of electrical resistivity of the ground, we will be capable of create a 3D map of thermal conductivities in the sub-soil for all the area of interest. This way, we are going to be able to choose the better areas for the boreholes, not just the thermal properties of them. We are going to have information about the cohesive state of the materials so we can project much better the drilling technique.

For the same initial conditions (energy needs, location, etc.), 2 different installations will be presented and discussed for comparison:

Scenario A: Installation designed without using the data from the *ERT*, all the data collected from bibliographical sources, tables, etc.

Scenario B: Installation designed using the *ERT* data to estimate the thermal conductivity and the ideal location for the boreholes. The additional data needed is obtained from the same sources as case A.

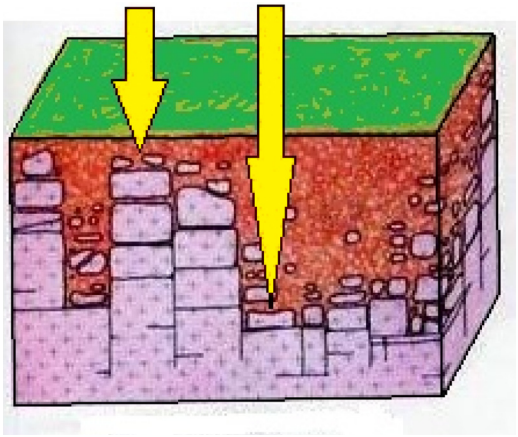

Fig. 1. Highly fractured granite environment, the arrows show the different materials we can find depending on the placement of the boreholes.

Table 1
Current accepted magnitude orders for electrical resistivities and thermal conductivities of rocks, soils and water.

Material	Resistivity (Ohm·m)	Thermal Conductivity[a] (W/m·K)
Igneous and metamorphic rocks		
Granite	$2 \times 10^3 \rightarrow 10^6$	1.5 → 5
Basalt	$10^3 \rightarrow 10^6$	1.5 → 2.5
Slate	$6 \times 10^3 \rightarrow 4 \times 10^6$	1.5 → 2
Marble	$10^2 \rightarrow 2.5 \times 10^8$	1.8 → 3
Quartzite	$10^2 \rightarrow 2 \times 10^8$	3 → 3.5
Sedimentary rocks		
Sandstone	$4 - 8 \times 10^3$	1.5 → 3.5
Shale	$20 \rightarrow 2 \times 10^3$	1.5 → 4
Siltstone	$50 \rightarrow 4 \times 10^2$	2.5 → 3
Limestone	$10^4 \rightarrow 10^5$	1.4 → 2.4
Soils and water		
Clay	1 → 100	0.5 → 3
Sedimentary soil	10 → 800	0.3 → 3
Freshwater	10 → 100	0.6
Seawater	0.2	0.6

[a] Some original data in Conductivity Units (CU) (Popov et al., 2003) (1 CU = 0.4184 W/mK) (Robertson, 1988).

2. Relation of electrical resistivity (ρ) to thermal conductivity (λ) and laboratory measurements

2.1. Relation of electrical resistivity (ρ) to thermal conductivity (λ)

In Table 1, we can observe that igneous and metamorphic rocks typically have high resistivity values (Robertson, 1988; Blázquez et al., 2018b). The resistivity of these rocks depends a lot on the degree of fracturing that they have and the percentage of water that fills the ground fractures.

We can assume that in the area of the project, the boreholes will be above the water table, so there will be no interaction with the groundwater level which is expected to be way down our installation (MAGNA, 2019).

It is noticeable from Table 1 that somehow the state of compactness of the different families of rocks tends to affect in an unfavorable way the thermal conductivity (for instance we can compare granite with sandstone).

The electric resistivity of granite type rocks behaves directly proportional to the altered state that they have (Kolditz, 1995).

On the other hand, the thermal conductivity of granite type rocks behaves inversely proportional to the level of alteration of the granite type rocks.

This behavior is partially due to the increase in clay content, which comes from feldspar, typical of the process of in-situ weathering of granites.

We will take samples to the laboratory from the project area to measure electrical resistivity and thermal conductivity, in order to establish the relationship.

Thermal conductivity of rocks depends on various factors including porosity, fracturing, mineral composition and structure. Many studies have demonstrated the significance of porosity and fracturing on rock thermal conductivity, and have shown that between these properties there exists a complicated relationship, which is particularly dependent on the pore space structure (Robertson, 1988).

Granite type rocks (such as adamellites) frequently suffer a disaggregation due to “in situ” weathering only (as in the present case) or by complete erosive processes with weathering and transport. In rocks

Fig. 2. A) KD2 Pro, (Decagon Devices, 2016) and sensor RK-1. (Range from 0.1 to 6 W/mK, accuracy 10%) B) Rock cores, 5 × 11.5 cm. We must drill to insert the needle (3.5 mm in diameter and 6 cm in length) and use thermal grease to improve the thermal contact C) Proctor compacted soil samples, (in situ water content preserved). D) Core samples extraction.

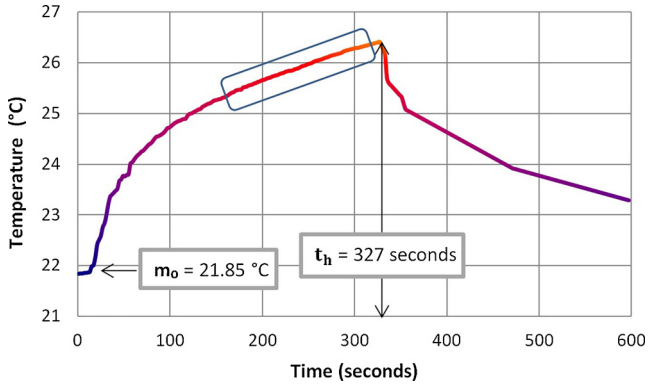

Fig. 3. Evolution of temperatures during the measurement process with KD2-PRO. The **blue** rectangle shows the area where the values for the linear regression in Fig. 4 are obtained (For interpretation of the references to colour in this figure legend, the reader is referred to the web version of this article).

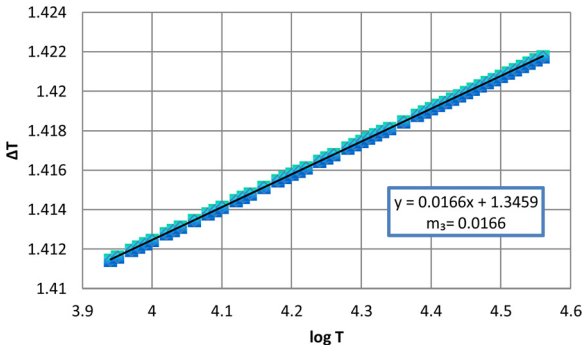

Fig. 4. Linear regression of temperature rise to logarithm of temperature.

composed of different large grain minerals (such as granite for example) the weathering attacks the first the weakest mineral. Especially the bonds between the minerals lose stability. In the end the rock is broken down to a set of loose grains.

In the process of weathering of the granites, clay materials from the disintegration of feldspars appear (with low thermal conductivity compared to sound granite rock. This, together with the fact that it increases the porosity and fracturing, causes the thermal conductivity to be reduced in the various stages of weathering of this type of rocks (Robertson, 1988).

At the same time, electric resistivity also decreases as metheorization progresses, partially due to the progressive appearance of clay based material (with higher electric conductivity than the solid granite rock and C = electrical conductivity in Siemens; C = 1/ρ; ρ= resistivity in ohm meters) from the feldspars. There is also the contribution of the moist in the fractures and porous which also helps in the reduction of electric resistivity (Samouëlian et al., 2005).

Our aim is to find a relation between these two magnitudes (thermal conductivity and electric resistivity from the tomography) in the study area. With this information, we will be able to identify the best places for the location of the boreholes in the well field, the ones with better thermal conductivity across their length. Better thermal conductivity also means more cohesive state in the subsoil in this kind of environments (Blázquez et al., 2018b). So in the 3d tomography we can also find information about the compactness of the ground in the area, allowing us to fit better the drilling method. Some problems in the drilling process will be avoided by selecting the proper method according to the type of rock formation we will find. In granite type rock environments, hammer drilling with air is the ideal technique. However if the ground is not compact enough, we can find several problems (subsidence, entrapment of the hammer, etc.). Conventional rotary drilling is the other method, much more suitable for soils and less compact materials than hammer drilling. This method usually is much more expensive than the previous one.

2.2. Laboratory Measurements

The equipment used for measuring thermal conductivities of samples in the laboratory was the thermal properties analyzer commercially known as KD2 Pro, developed by Decagon Devices (Decagon Devices,

Table 2
Laboratory measurements from samples collected in the project´s area.

Sample	Qualitative Description	Measure	Thermal Conductivity (W/m·K)	Mean	Std. Deviation	Electrical Resistivity (Ω·m)	Mean	Std. Deviation
Grus 1	Altered	M1	1.423	1.490	0.092	72.52	74.28	2.54
		M2	1.421			77.25		
		M3	1.582			76.23		
		M4	1.503			71.12		
Grus 2	Altered	M1	1.435	1.499	0.096	65.45	65.89	2.18
		M2	1.497			68.23		
		M3	1.514			67.36		
		M4	1.584			62.54		
Altered 1	Partially Altered	M1	1.862	1.899	0.024	1092.4	1177.7	78.41
		M2	1.914			1192.3		
		M3	1.926			1127.7		
		M4	1.895			1298.5		
Altered 2	Partially Altered	M1	2.315	2.196	0.11	1650.3	1691.8	71.44
		M2	2.012			1725.2		
		M3	2.255			1602.7		
		M4	2.203			1789.6		
Adamellite A	Sound Granite Rock	M1	2.694	2.619	0.050	2230.3	2188.2	39.63
		M2	2.562			2124.8		
		M3	2.587			2187.5		
		M4	2.634			2210.3		
Adamellite B	Sound Granite Rock	M1	2.974	2.954	0.025	2324.7	2361.8	42.78
		M2	2.946			2410.8		
		M3	2.981			2397.4		
		M4	2.916			2314.1		

*Sample selection was carried out by visual inspection “in-situ” from the study area.

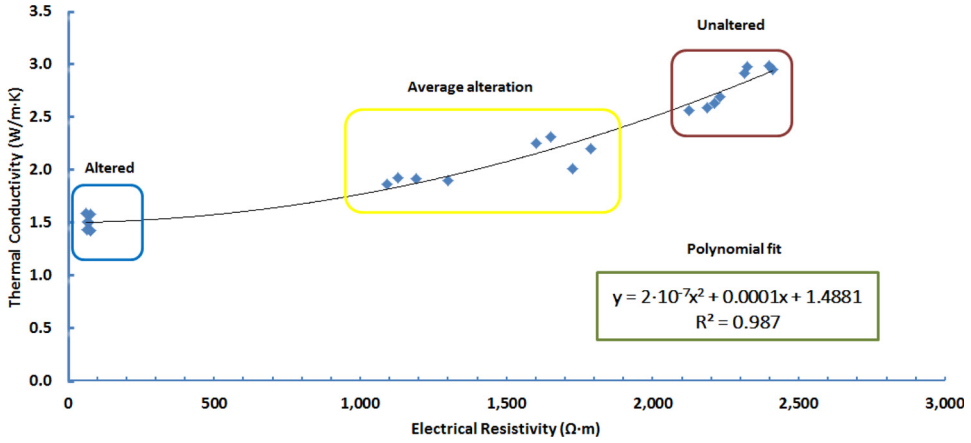

Fig. 5. Thermal conductivity vs. electrical resistivity (data from Table 1).

2016). It is constituted by a portable controller and a certain sensor (RK-1) (Fig. 4) commonly used in geothermal practice and usually known as “needle probe” that makes possible the measuring of the thermal conductivity (KD2 Pro, 2016) (Fig. 2).

The measurement operation is based on the infinite line heat source theory and calculates the thermal conductivity by monitoring the dissipation of heat from the needle probe. Heat is applied to the needle for a set heating time, t_h and temperature is measured in the monitoring needle during heating and for an additional time equal to t_h after heating (Fig. 3).

The temperature during heating is computed from Eq. (1).

$$T = m_0 + m_2 t + m_3 ln t \quad (1)$$

Where:

m_0 is the ambient temperature during heating.

m_2 is the rate of background temperature drift.

m_3 is the slope of a line relating temperature rise to logarithm of temperature.

Eq. (2) represents the model during cooling.

$$T = m_1 + m_2 t + m_3 ln \frac{t}{t - t_h} \quad (2)$$

The thermal conductivity is computed from Eq. (3).

$$K = \frac{q}{4m_3} \quad (3)$$

q is the heat flux applied to the needle probe for a set time (Fig. 4).

In this study, the RK-1 probe has been used to measure the thermal conductivity of the different materials collected from the area of study. This probe is capable of measuring the thermal conductivity between the range of 0.1 and 6 W/mK and ± 10% of accuracy.

From samples collected in the area of the project (Fig. 2 shows description of the samples) we have measured:

A.) Thermal conductivity, using KD2-Pro devices described above.
B.) Electric resistivity, with a regular electric device.

Table 2 shows the measures of 3 types of samples collected from the area of the project:

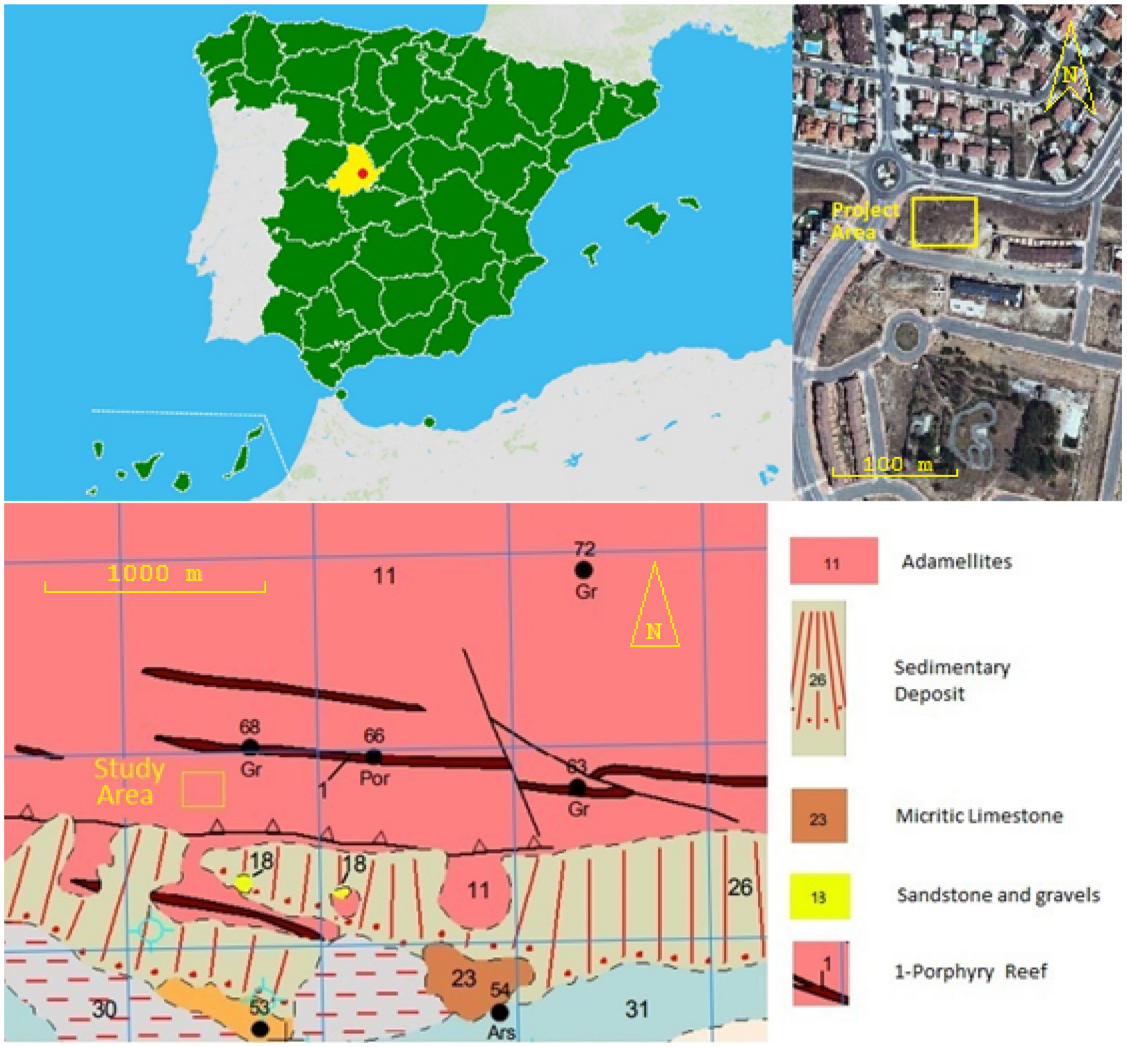

Fig. 6. Location and geology of the project´s area.

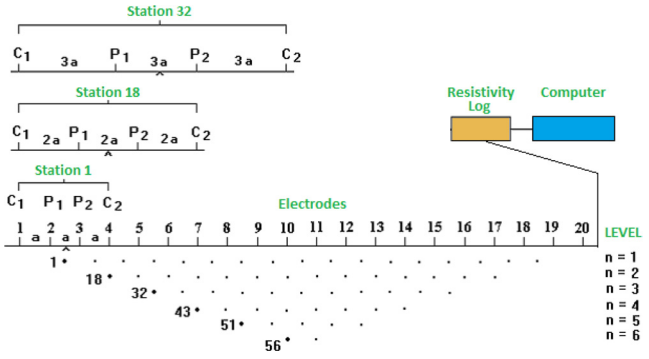

Fig. 7. ERT field data capture diagram of apparent resistivity (later to be processed to obtain real resistivity and, due to this, the geological structure).

- Grus (from the in-situ metheorization of the granite type environment). Samples compacted, Proctor compaction with humidity corresponding to the ascendant phase of the proctor essay (Bjerrum et al., 1973). The original conditions of humidity of the samples were preserved.
- Medium altered adamellites (intact samples cored and drilled).
- Adamellites (solid rocks, cored and drilled).

R is used as a proxy for λ and lab results show that λ can be estimated to ± 0.15 W /m·K. One could also estimate λ from rock appearance: sound granite = 2.5–3.0 W/m·K, and altered granite = 1.6–2.2 W/m·K.

With the above data we can establish the following relationship shown in Fig. 5

3. Site description

The investigated area is located within the Spanish region of Ávila, in the Central System Mountains, the predominant materials being igneous rocks belonging to the large tectonic blocks in which the Hercynian massif was divided during alpine folds (MAGNA, 2019) (Fig. 5).

The study area is entirely within the area mapped as adamellite (a coarse-crystalline intrusive igneous rock composed mostly of quartz, orthoclase and plagioclase). Several degrees of weathering and disintegration are observed at the surface:

1 Grus (sands and clays), products of the “in situ” mechanical and chemical disintegration of the granites ", the thickness of this altered zone is very variable, according to geological information, from 1 or two to 45 m (Directive (EU), 2019).
2 Outcrops of altered weathered adamellite in-situ and cohesive material.
3 Rocky outcrops of sound solid, granite, fracture spacing typically

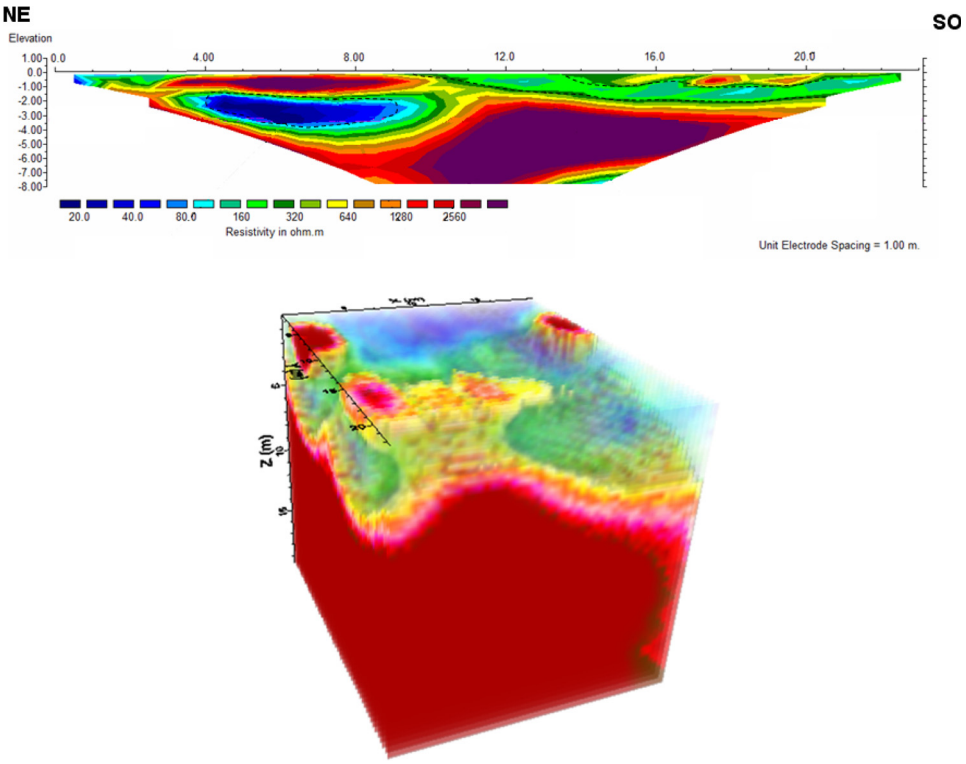

Fig. 8. Sample 2D and 3D models of real resistivity and depth obtained from RES2DINV and RES3DINV software.

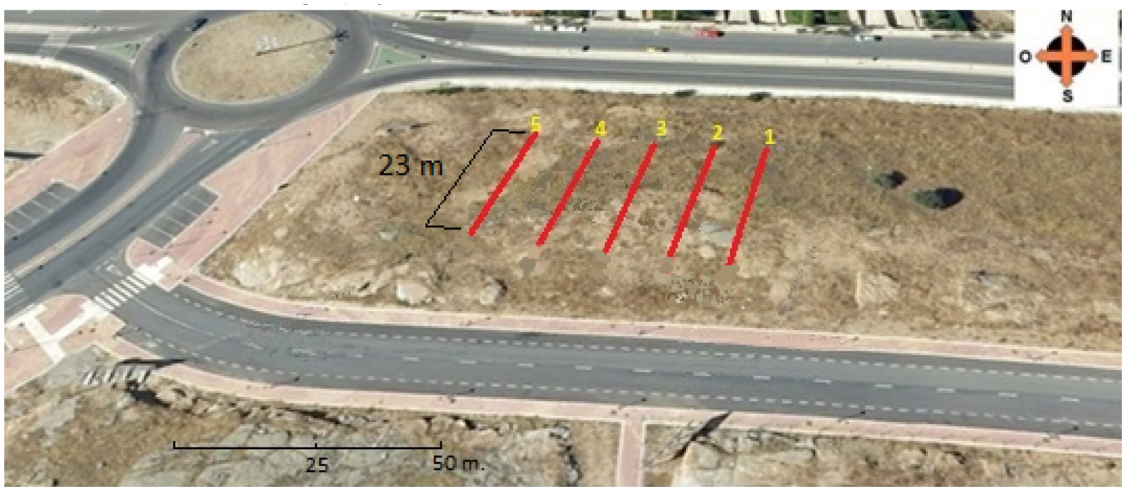

Fig. 9. 2D profiles location.

Table 3
Location of the extreme lines 1 and 5 of the 2D profiles.

Line		North Point	South Point
1	Latitude	40° 39' 23.17'' N	40° 39' 22.50'' N
	Longitude	4° 40' 39.48'' W	4° 40' 39.62'' W
5	Latitude	40° 39' 23.39'' N	40° 39' 22.60'' N
	Longitude	4° 40' 40.90'' W	4° 40' 41.23'' W

around several meters (MAGNA, 2019) (Fig. 6).

4. Electrical resistivity tomography (ERT), survey method

The Electrical resistivity tomography (*ERT*) is a research technique for the characterization of the subsoil in such important fields as mining, hydrogeology, underground environmental pollution, agricultural pollution, modern archeology, geotechnology, and in general the location of structures and complex anomalies usually sub superficial, both geological and anthropic.

The Electrical Resistivity Tomography consists of measuring the apparent resistivity (ρ_a) of the terrain (Eq. (1)) at different depths,

$$\rho_a = K\frac{\Delta V}{I} \quad (1)$$

Where K is constant for each device (a geometric factor), ΔV is the potential difference measured on the ground and I the current injected.

We use a tetra-electrode device with a constant separation between electrodes called "*a*", varying the distances between the pairs of emitting-receiving electrodes by multiples of a value called "*n*". As a result, a section of ρ_a at several levels "*n*" in depth will be obtained; data that are subsequently processed through mathematical investment algorithms

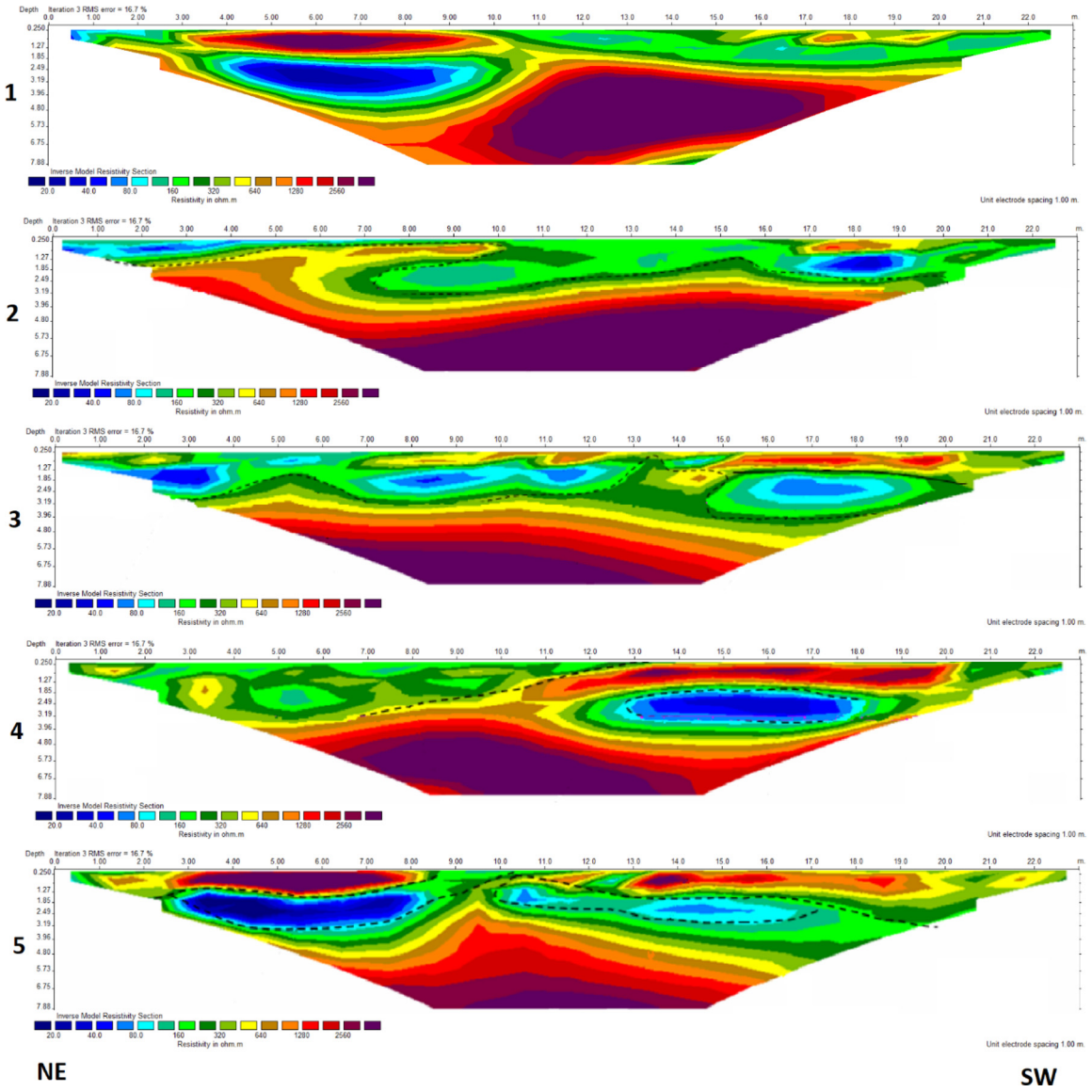

Fig. 10. 2d profiles processed with RES2DINV software (error 16.7%).

(Fig. 7) (Keller and Frischknecht, 1966).

With this apparent resistivity data, a software processing process is carried out using 2D and 3D modeling. Introducing the apparent resistivity and distance/depth data in an inversion program (RES2DINV-RES3DINV) (Geotomo Software, 2019) we can obtain the electrical surface profiles for the different materials at different depths.

The software returns as a result an "Image of real resistivity and depth" (Fig. 8). Those results should be checked with geological information of the area (field observations, drill data, etc.).

The inversion of the data returns as a result a section or block (as shown in Fig. 3) of resistivity, which is usually a very good approximation of the model of real resistivity vs. depth of the subsoil.

5. ERT result and thermal conductivity structure

5.1. Tomography lines location

In the figure (Fig. 9), we can see the position of the 2D electrical resistivity profiles used to model the 3D tomography (Table 3).

5.2. ERT results

Fig. 10 shows 2D profiles processed with RES2DINV to show the inversion of measured values to subsurface resistivity. The RES2DINV programs use the smoothness-constrained Gauss-Newton least-squares inversion technique (Sasaki, 1992) to produce a 2D model of the subsurface from the apparent resistivity data. The process is now completely automatic; the user does not have to supply a starting model (Olayinka and Yaramanci, 2000).

In Figs. 11 and 12 we can see processes trough the RES3DINV software. The program uses also the smoothness-constrained least-squares inversion technique to produce a 3D model of the subsurface from the apparent resistivity data.

Fig. 11 shows horizontal profiles from the process of the RES2DINV data of the *ERT*, the modeled extension of these profiles to a 3D object is shown in Fig. 12.

In Fig. 12 we can see the 3d model complete of the location for the well field, It´s a 20 × 20 × 20 m cube that will allow us to establish the better location for our boreholes (we will have to balance the distance against the improvement in the thermal conductivity of the different solutions modeling the different possibilities).

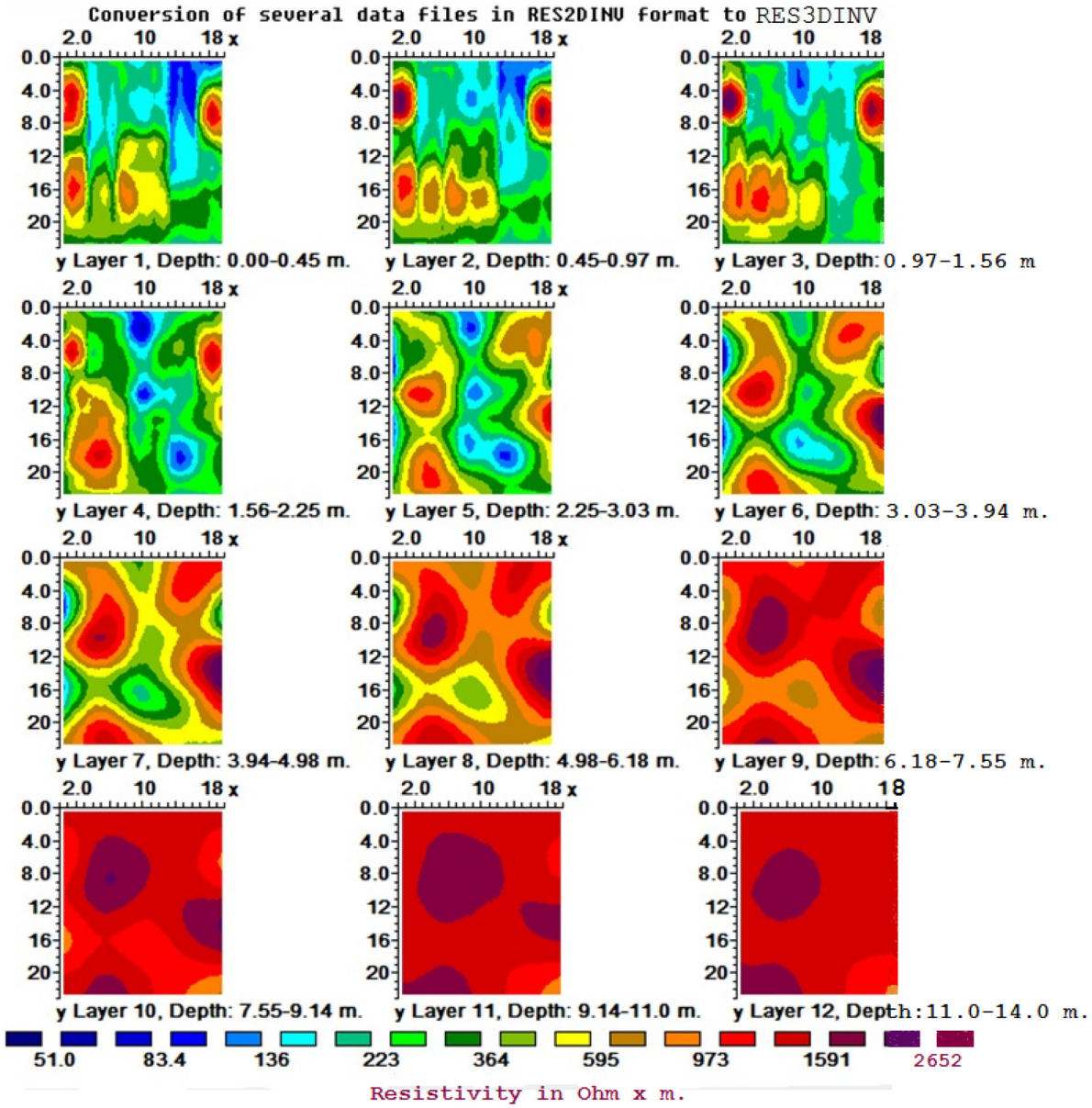

Fig. 11. 3D processing, horizontal sections, RES3DINV program (numbers on margins are x and y coordinates of survey in meters) RMS error 19.2%.

5.3. Thermal conductivity structure

According to the measures in chapter 2, we can establish the thermal conductivity of the subsoil in the area of the project (Fig. 13).

This will allow us to find the best locations for our wells, and also to estimate the thermal conductivity around each one in order to be more accurate in the calculus of the length of the boreholes.

6. Project design

Our project is based in the design of a low enthalpy geothermal system in order to provide 31.245 MW h per year (only in heating function).

It´s an actual project to be implemented in the area described in chapter 3 (Table 4).

As mentioned in the introduction, we will design the well field in two scenarios:

Scenario A: Installation designed without using the data from the *ERT*, all the data collected from theoretical sources, tables, etc. Specifically, thermal conductivity of the ground (λ) is assigned based on an assumed lithology of the ground and using published laboratory measurements (Blázquez et al., 2017a). This scenario generally results in a wide separation of boreholes.

Scenario B: Installation designed using the ERT data to estimate the thermal conductivity and the ideal location for the boreholes. The other necessary inputs will be taken from the same sources as scenario A.

The project is based on a vertical closed loop geothermal system, in each of the two scenarios studied it´s expected that we will have different fluid temperatures due to the different designs of the well field. We are selecting the same heat pump for both scenarios based on the energy needs, which are the same. However, the performance of this heat pump will be different in each scenario because it depends on the temperature of the thermal fluid from the well field if all other circumstances are the same: BS EN 14825:2016 “Air conditioners, liquid chilling packages and heat pumps, with electrically driven compressors, for space heating and cooling. Testing and rating at part load conditions and calculation of seasonal performance”.

The area for the well field consists on a 20 × 20 square meter surface, with no other restrictions for the location of the boreholes applicable.

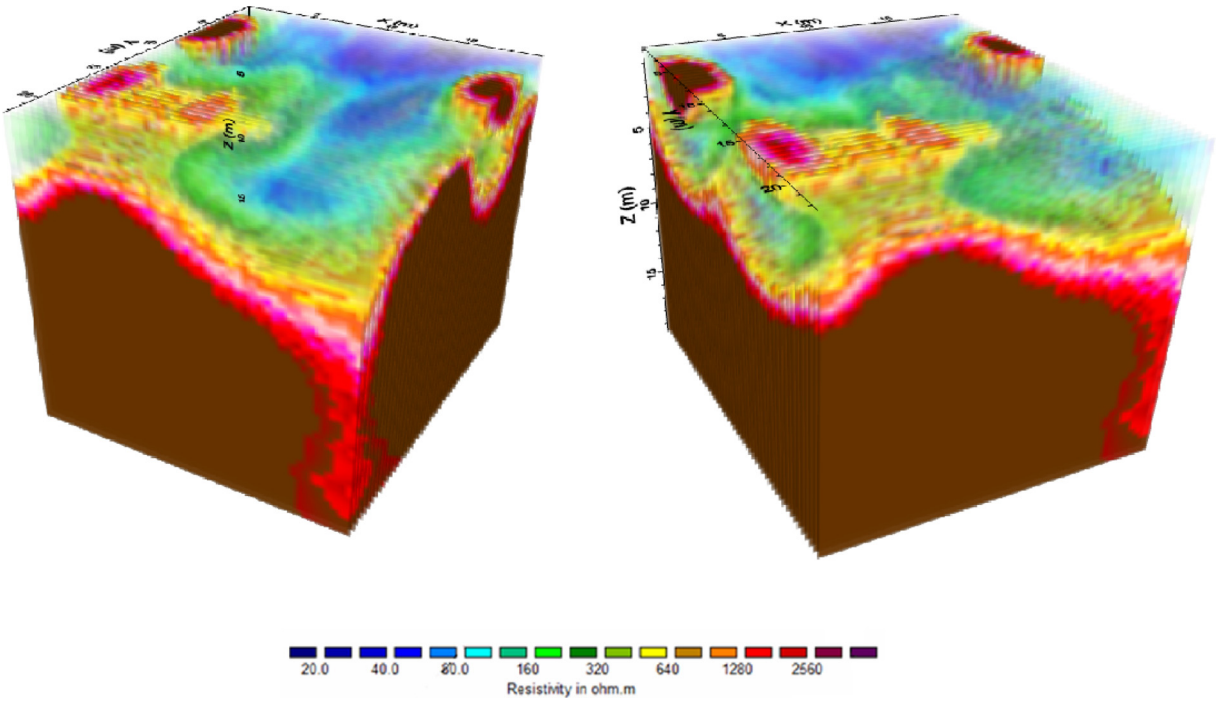

Fig. 12. 3D processing (20 × 20 × 20 m cube).

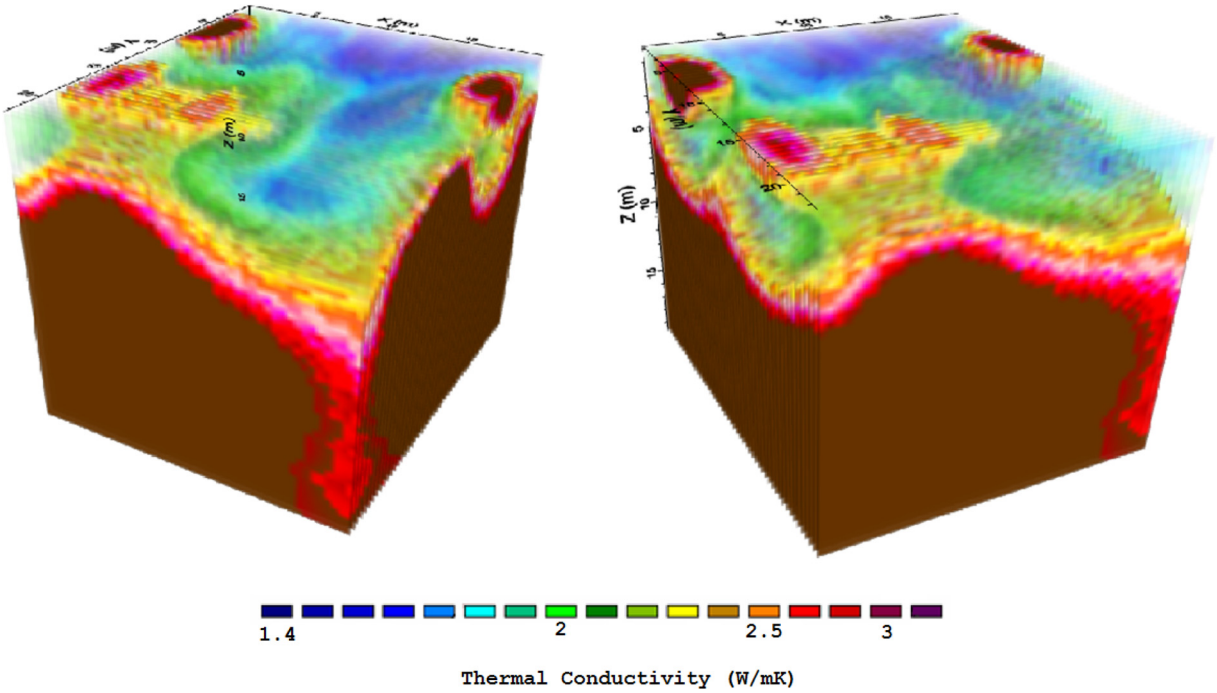

Fig. 13. Thermal Conductivity Structure of the subsoil (W/mK).

Both scenarios will be modeled using Earth Energy Designer (EED) geothermal software (EED software created by BLOCON, 2019). EED is a PC-program for vertical borehole heat exchanger design. It is used in everyday engineering work for design of ground source heat pump system (GSHP) and borehole thermal storage. It can be purchased online in https://buildingphysics.com/.

6.1. Scenario A. Design without the ERT information

Here we assign the value of the heat conductivity of the ground (λ) based on geological information, according to which we can assess λ = 1.9 W/m·K (Blázquez et al., 2017a; Robertson, 1988).

We have a 20 × 20 m field, and no other placing restrictions are applied to the optimization process.

Results for the proposed solutions are shown in Table 5.

We would probably choose the 2-well proposal due to the convenience the drilling company's rig which is usually limited to a depth of 100 m. Under these circumstances the mean temperatures of the geothermal fluid (the fluid in the closed ground loop) evolve as shown in Fig. 8:

They are acceptable for the working range of our heat pump (above −5 °C), nevertheless there is expected a reduction of the C.O.P as time

Table 4
Monthly distribution of the energy needs from the ground.

Month	Energy (MWh)	Percentage (%)	Mean monthly temperature (°C)[a]
January	3.887	15.5	2.7
February	3.712	14.8	4.1
March	3.135	12.5	6.9
April	2.632	10.6	9
May	2.483	9.9	12.2
June	0.000	0.0	17.1
July	0.000	0.0	20.7
August	0.000	0.0	20.1
September	1.530	6.1	16.7
October	2.182	8.7	11.1
November	2.934	11.7	6.1
December	3.611	14.4	3.7

[a] Data from "Agencia Estatal de Meteorología (AEMET), Ministry for Ecologic Transition, Spanish Government".

Table 5
Proposed solutions by geothermal software based on 25 years simulation (EED software).

Number of Wells	Type	Spacing (m)	Depth (m)	Total Length (m)
1	Single	–	165	165
2	1 × 2 Line	20	94	188
2	1 × 2 Line	18	95	190
2	1 × 2 Line	17	96	192
2	1 × 2 Line	15	99	198

passes due to the descent of the fluid temperature (Fig. 14).

6.2. Scenario B, design using the information from the ERT

According to the ERT data, we consider the best location for the boreholes, with the idea of using the correspondence between electric resistivity and heat conductivity to esteem this one in the design process.

It´s necessary to have in mind the results from scenario A, this way we already know the number of wells required (approximately), in order to locate them.

Working with the 3D model, offered by the simulation of the RES2DINV-RES3DINV software, based in the ERT data, we can now choose how to locate the boreholes in order to obtain the better possible heat conductivity of the ground and also the most convenient subsoil for the drilling process.

We must take into account the separation between the boreholes, in this case as far from each other as possible (Beier et al., 2011).

Fig. 15 shows two views of the locations selected for each one of the boreholes.

The estimation of the thermal conductivity (λ) of the ground for both boreholes can be calculated with the polynomial fit from the Fig. 5 using data from the electrical resistivity of each section of the projected borehole.

$$\lambda = 2 \cdot 10^{-7} \rho^2 + 0.0001\rho + 1.4881 \quad (5)$$

$$R^2 = 0.987 \quad (6)$$

Considering each section length and electrical resistivity from the ERT we can obtain the thermal conductivity for the whole borehole (λ_B):

$$\lambda_B = \sum_{1}^{n} \lambda_i \times \frac{l_i}{L} \quad (7)$$

We must bear in mind that we cannot be sure about the length of the wells, this will come with the simulation in EED software, but as far as the λ is needed as an input of : the software we have better confidence to assess the borehole length than in scenario A.

Since the 3D model shows unaltered adamellite all through the wells except for a few meters in the upper section (less than 5 m in each case), and we are expecting lengths of around 70 m and up, we will obtain a much better value for λ than in the previous case. All this with sufficient reliability to trust the reduction in the length of the boreholes from ˜95 m in scenario A to ˜70 m in scenario B.

In Table 6 are collected the estimated values of the characteristics of the wells from previous data:

With the thermal conductivity estimated and all the other parameters of the project being the same, the design of the well field proposed now by the simulation is shown in Table 7.

In this scenario it´s meaningless to show the other possibilities offered by the software, because we are focusing on our fixed location with the ground conditions shown above and the distance between the wells estimated from the 3D model.

The development of the temperatures of the fluid is shown in Fig. 16.

As we can see, we have achieved a considerable reduction in the drilling length (190 m – 140 m = 50 m), as well as an improvement in the behavior of the geothermal fluid temperatures.

7. Economic study of these types of projects

The cost of an ERT (Electrical Resistivity Tomography) in the area of

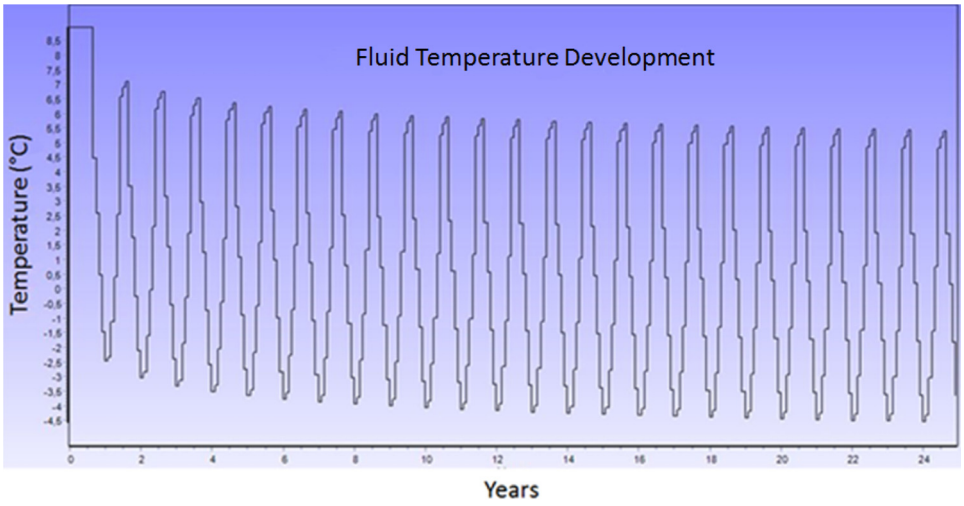

Fig. 14. Scenario 1, fluid´s temperature evolution (25 years).

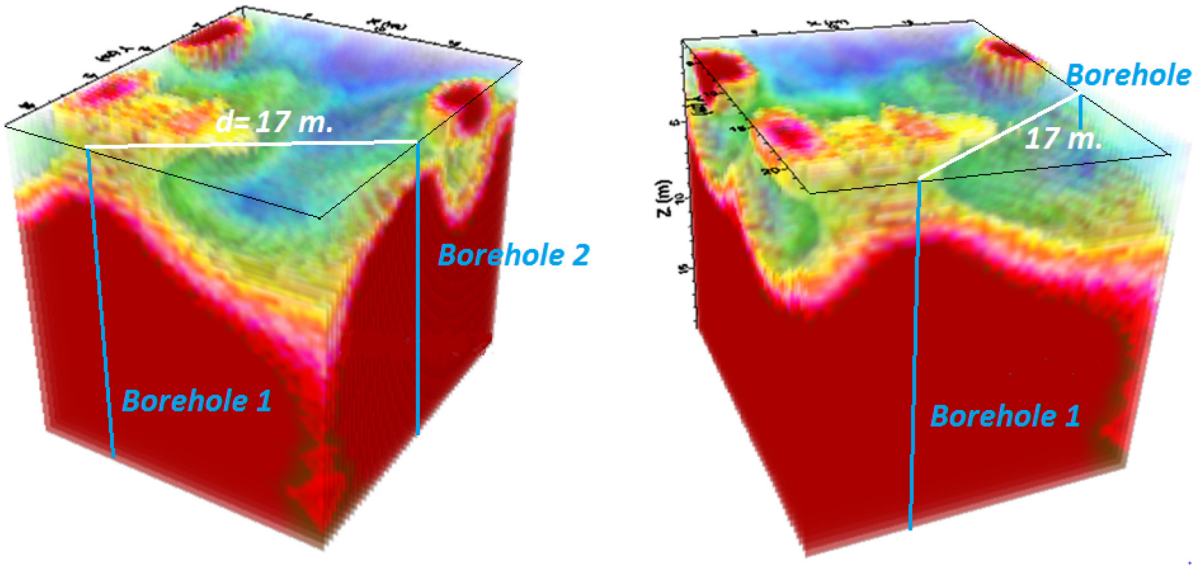

Fig. 15. Locations selected for each one of the boreholes (2 views).

Table 6
Heat conductivity estimation for the boreholes.

Borehole 1			Borehole 2		
Depth	Electrical Resistivity (Ω·m)	Thermal Conductivity (W/m·K)	Depth	Electrical Resistivity (Ω·m)	Thermal Conductivity (W/m·K)
0-5 m.	635.5	1.81	0-3 m.	523.3	1.75
5- end	2275.0	2.8	3-end	2275.0	2.8

Ground thermal conductivity for each borehole (W/m·K).

Borehole 1	Borehole 2
2.72	2.75

Combined thermal conductivity for the well field (W/m·K).
2.74

Table 7
EED's optimization well field proposal.

Number of Wells	Type	Spacing (m)	Depth (m)	Total Length (m)
1	Single	–	130	130
2	1 × 2 Line	17	70	140

a low enthalpy geothermal project may be around 3000–4000 €. More or less the same cost of a Thermal Response Test (TRT) in one or two initial wells of the well field (Técnicas Geofísicas, 2019).

In this project, we have implemented the ERT information for academic purposes, because the small size of the well field does not justify the expense. However, in much bigger projects, a 25% reduction of the drilling costs could make worthy the investment in an ERT of the area (for these particular geological environments).

Including the information from the ERTs in our design process we have improved dramatically the accuracy of the location of the wells in the well field (taking into account the better drilling conditions in the second design due to the higher amount of solid rock in the field which is much better in our proposed drilling method), also the drilling length has been reduced in a 25.5%.

We estimate the initial investment of the project in about 25,000 euros. Considering that the price per meter of drilling for the chosen system is about 45€, a reduction of 48 m represents a saving of 2160€. This means an 8% reduction in the initial investment (Fig. 17).

The modeled behavior of the installation in 25 years, based mainly on the mean temperatures of the fluid from the well´s field, reach an important improvement as shown in Figs. 11 and 13. We can see in Fig. 11 that the Temperature reaches −4.5 °C, however in the second scenario (Fig. 13) Temperature descends till −0.5 °C only.

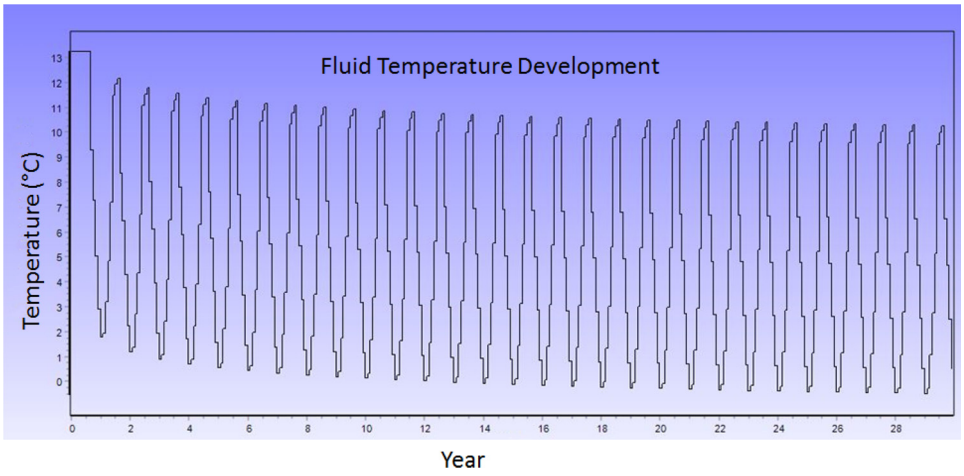

Fig. 16. Scenario 2, fluid´s temperature development (25 years).

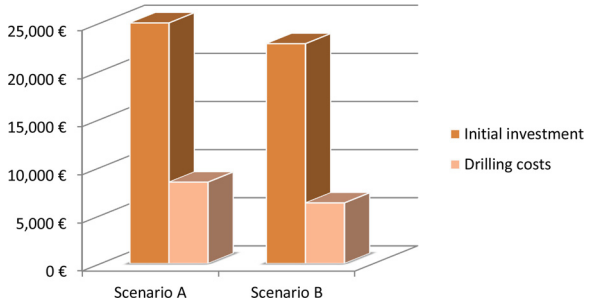

Fig. 17. Economic comparison between scenarios.

The temperature of the fluid is quite important when we are trying to improve the performance of any geothermal system, we must remember that it is directly proportional to the coefficient of performance of the heat pump (even it is mandatory to declare the operating temperatures of the heat pump when we are offering the COP (CEN - EN 16147/2017, 2019)).

Taking this into account we can estimate the difference in annual cost from the heat pumps working in each scenario. The temperatures to estimate the COP in each case will be the mean temperature for the 25 years period of simulation see the next Figs. 18 and 19.

The COPs for the heat pump at those mean temperatures are shown at table 10. Although scenario A is not real, since we have underestimated the thermal conductivity of the ground, gives us an idea of the deviation in the forecasts that we would be committing when projecting the geothermal installation without the ERT data (Table 8).

8. Conclusions

There are some geological structures (Fig. 1), where it´s possible to find a great difference in the material compactness with quite low horizontal displacement (Dewandel et al., 2006). This is an attempt to apply geophysical methods (based on electric resistivity tomography) to help us in finding the best location for the wells in this type of areas. Constructing a 3D model of the ground in the area of the project will allow us to locate the wells in the best possible situations (from the thermal point of view) as well as to avoid difficult areas for the drilling process.

This particular project where we have included the ERT is probably too small to see a clear economic return of the investment on a geophysical survey, however, with a 25% saving in the drilling length (in this case) it´s easy to conclude that there could be much bigger projects in these type of ground that could benefit from these type of technique.

The increase of performance of the well field for the geothermal system that we can obtain also means an important saving in electric power thorough the life of the installation. This becomes more and more important with the increase of the geothermal system´s electric power installed. The bigger the heat pump is we have better economic results by reducing the annual energy costs.

Apart of the savings in the drilling length we can obtain there is also the possibility of choosing the best locations for the wells from the drilling point of view. This is not possible with the TRT test, since it does not offer us a general view of the geological structure of the area. Choosing the correct drilling method based on the previous knowledge of the geology of the area has two main advantages:

1 Prevents failures during the drilling process of the well field.
2 Makes possible to select the best drilling method in each case.

The inclusion of geological 3D models in the process of designing low enthalpy geothermal systems will become more and more popular in the future. This will allow the designers to model the thermal interaction of the ground with the wells of the project.

We expect that more and more high energy demand geothermal projects will include geophysical surveys (depending on the geology of the area) to complement the usual thermal response test which now are quite common.

Acknowledgments

Authors would like to thank the Department of Cartographic and Land Engineering of the Higher Polytechnic School of Avila, University of Salamanca, for allowing us to use their facilities and their collaboration during the experimental phase of this research. Authors also want to thank the University of Salamanca and Santander Bank for providing a pre-doctoral Grant (Training of University Teachers Grant) to the corresponding author of this paper what has made possible the realization of the present work.

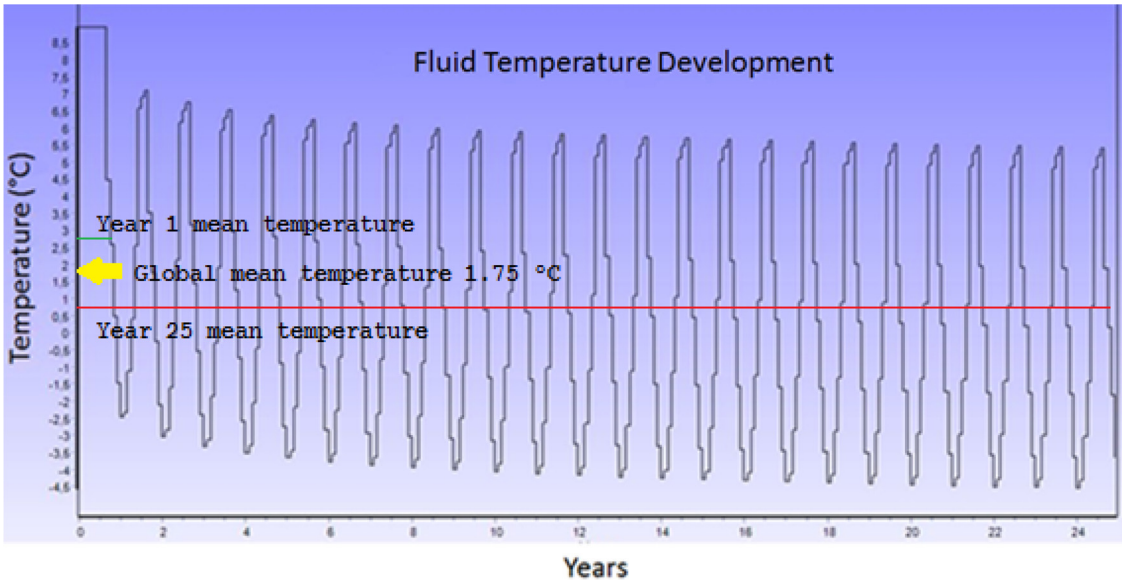

Fig. 18. Mean temperature for scenario A.

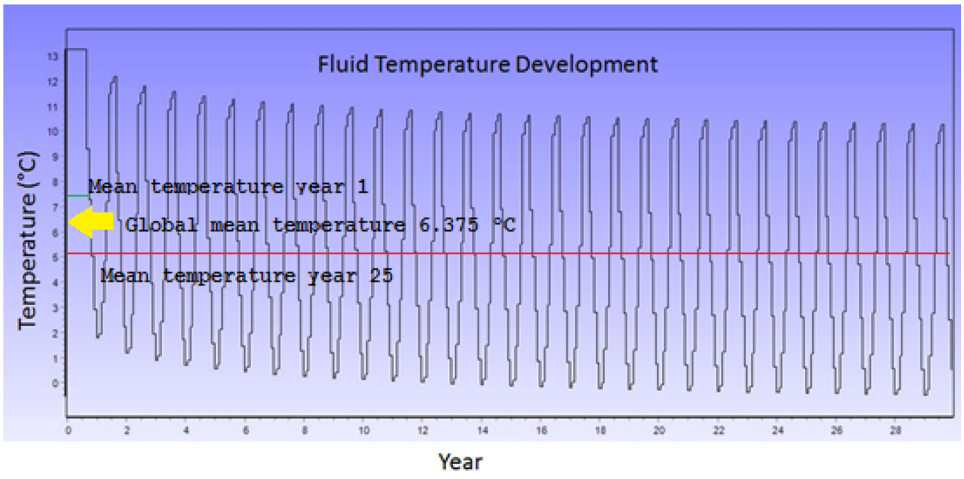

Fig. 19. Mean temperature for scenario B.

Table 8
Operational cost for heat pumps working (energy prize: 0.14 euro/kwh).

Scenario	Global mean temperature (°C).	COP	Energy per year. (kwh)	Cost (euros/ first year)
A	1.75	4.1	7620.73	1066.90
B	6.38	4.6	6792.39	950.93

References

Beier, R.A., Smith, M.D., Spitler, J.D., 2011. Reference data sets for vertical borehole ground heat exchanger models and thermal response test analysis. Geothermics 40 (1), 79–85.

Bjerrum, L., Casagrande, A., Peck, R.B., Skempton, y.A.W., Wiley, John, Sons Terzaghi, K., 1973. Mechanism of Landslides From Theory to Practice in Soilmechanics. V III.

Blázquez, C.S., Martín, A.F., Nieto, I.M., García, P.C., Pérez, L.S.S., Aguilera, D.G., 2017a. Thermal conductivity map of the Avila region (Spain) based on thermal conductivity measurements of different rock and soil samples. Geothermics 65, 60–71.

Blázquez, C.S., Martín, A.F., Nieto, I.M., García, P.C., Pérez, L.S.S., González-Aguilera, D., 2017b. Analysis and study of different grouting materials in vertical geothermal closed-loop systems. Renew. Energy 114, 1189–1200.

Blázquez, C.S., Martín, A.F., Nieto, I.M., González-Aguilera, D., 2018a. Economic and environmental analysis of different district heating systems aided by geothermal energy. Energies 11 (5), 1–17.

Blázquez, C.S., Martín, A.F., García, P.C., González-Aguilera, D., 2018b. Thermal conductivity characterization of three geological formations by the implementation of geophysical methods. Geothermics 72, 101–111.

CEN - EN 16147/2017, 2019. Heat Pumps with Electrically Driven Compressors - Testing, Performance Rating and Requirements for Marking of Domestic Hot Water Units.

Dewandel, B., Lachassagne, P., Wyns, R., Maréchal, J.C., Krishnamurthy, N.S., 2006. A generalized 3-D geological and hydrogeological conceptual model of granite aquifers controlled by single or multiphase weathering. J. Hydrol. (Amst) 330 (1–2), 260–284.

Directive (EU), 2019. 2018/410 Of the European Parliament and of the Council of 14 March 2018 Amending Directive 2003/87/EC to Enhance Cost-effective Emission Reductions and Low-carbon Investments, and Decision (EU) 2015/1814.

EED software created by BLOCON, 2019. EED Software Created by BLOCON Company Dedicated to Create Software About Heat Transfer and Ground Heat. https://buildingphysics.com/eed-2/.

RES2DINVx32/x64/ RES3DINVx32/x64- 2D and 3D Resistivity & Ip Inversion Software. Geotomo Software].

KD2 Pro, 2016. Thermal Properties Analyzer. Decagon Devices, Inc. Version: February 29.

Keller, G.V., Frischknecht, F.C., 1966. Electrical Methods in Geophysical Prospecting.

Kolditz, O., 1995. Modelling flow and heat transfer in fractured rocks: conceptual model of a 3-D deterministic fracture network. Geothermics 24 (3), 451–470.

Kukkonen, I., Lindberg, A., 1995. Thermal Conductivity of Rocks at the TVO Investigation Sites Olkiluoto, Romuvaara and Kivetty (No. YJT–95-08). Nuclear Waste Commission of Finnish Power Companies.

Liou, J.C., Tien, N.C., 2016. Estimation of the thermal conductivity of granite using a combination of experiments and numerical simulation. Int. J. Rock Mech. Min. Sci. 81, 39–46.

Geological and Mining Institute of Spain (IGME), 1972–2003. Geological MationalMapping (MAGNA).

Olayinka, A.I., Yaramanci, U., 2000. Use of block inversion in the 2-D interpretation of apparent resistivity data and its comparison with smooth inversion. J. Appl. Geophy. 45 (2), 63–81.

Popov, Y., Tertychnyi, V., Romushkevich, R., Korobkov, D., Pohl, J., 2003. Interrelations between thermal conductivity and other physical properties of rocks: experimental data. Thermo-Hydro-Mechanical Coupling in Fractured Rock. pp. 1137–1161 Birkhäuser, Basel.

Robertson, E.C., 1988. Thermal properties of rocks. U. S. Geological Survey Open-File Report 88-441. pp. 97.

Samouëlian, A., Cousin, I., Tabbagh, A., Bruand, A., Richard, G., 2005. Electrical resistivity survey in soil science: a review. Soil Tillage Res. 83 (2), 173–193.

Sanner, B., Karytsas, C., Mendrinos, D., Rybach, L., 2003. Current status of ground source heat pumps and underground thermal energy storage in Europe. Geothermics 32 (4–6), 579–588.

Sanner, B., Hellström, G., Spitler, J., Gehlin, S., 2005. Thermal response test–current status and world-wide application. April. Proceedings World Geothermal Congress 24–29.

Sasaki, Yutaka, 1992. Resolution of resistivity tomography inferred from numerical simulation. Geophys. Prospect. 40, 453–463.

Signorelli, S., Bassetti, S., Pahud, D., Kohl, T., 2007. Numerical evaluation of thermal response tests. Geothermics 36 (2), 141–166.

Sundberg, J., Back, P.E., Ericsson, L.O., Wrafter, J., 2009. Estimation of thermal conductivity and its spatial variability in igneous rocks from in situ density logging. Int. J. Rock Mech. Min. Sci. 46 (6), 1023–1028.

Técnicas Geofísicas, 2019. S.L. Engineering Consulting.